Eng. & Tech. Journal, Vol. 29, No.5, 2011

Aerodynamic Parameters Analysis of Transonic Flow Past Unswept and Swept Wings

Raad Shehab Ahmed*

Received on:2 /4/ 6/2010
Accepted on: 3/3/2011

Abstract

The transonic flow past unswept and swept wings has been studied. For this purpose the transonic potential flow equation is solved for inviscid compressible flow. The shock waves are replaced by discontinuities across which the entropy is conserved. The velocity field and pressure coefficients are estimated as function of free stream Mach number. The results show the effect of free stream Mach number on shock waves location and the velocity field around the wing section. The Euler solution and potential flow solutions are identical at subsonic flow; however, at supersonic flow the potential theory can no longer predict the flow field correctly. The results show the important effect of sweep angle on the value of the critical Mach number for wings. By using Visual foil plus the pressure distribution and lift coefficient and Mach contours for flow Past a NACA 0012 airfoil can be predicted.

Keywords: Aerodynamic parameters, Transonic flow, Unswept and swept wings, Shock wave of wings

تحليل عوامل الايروديناميكية لجريان حول صوتي على الاجنحة المتراجعة والمستقيمة

الخلاصة

تم دراسة الجريان حول الصوتي عبر اجنحة متراجعة وغير متراجعة لهذا الغرض تم حل معادلة الجهد لجريان حول صوتي انضغاطي غير لزج . الموجات الصدمية تم استبدالها بقطوعات وعبرها تم الحفاظ على الانتروبي (العشوائية) . حقل السرعة ومعامل الضغط تم تخمينها لدالة من عدد ماخ للتيار الحر . النتائج تبين تاثير عدد ماخ للتيار الحر على موقع الموجة الصدمية وحقل السرعة حول مقطع الجناح . ان حل اويلر وحلول التيار الجهدي متشابهة تماماً للجريان دون الصوتي . على اية حال , عند جريان فوق صوتي فان نظرية التيار الجهدي لايمكنها بعد ذلك من تخمين حقل الجريان بصورة صحيحة . النتائج تبين التاثير المهم لزاوية التراجع على قيمة رقم ماخ الحرج للاجنحة . باستخدام برنامج فيشوال فويل بلاس (منظور المطيار الحقيقي) التوزيع الضغطي ومعامل الرفع وحدود ماخ للجريان يمكن تخمينها .

Nomenclature

Symbol	Unit Description	Unit
C_D	Drag coefficient	-
C_{DI}	Induced drag coefficient	-

*Machines and Equipments Engineering Department, University of Technology/ Baghdad

C_L	Lift coefficient	-
c_p	Surface Pressure Coefficient	-
M	Mach number	-
M_{CC}	Crest critical Mach number	-
M_{DD}	Drag divergence Mach number	-
M_{DIV}	Drag rise Mach number	-
P	pressure	N/m^2
P_O	Stagnation pressure	N/m^2
$P\infty$	Free stream pressure	N/m^2
R_e	Reynolds number	
T	Static pressure	K˚
T_O	Stagnation temperature	K˚
t	Thickness	m
t / c	Thickness to Chord Ratio	-
η	Span Location (% Span Length)	m
γ	Specific Heat Ratio	-
υ	Y velocity component	m/s

1. Introduction

Transonic flow past wings is the flow field at free stream Mach number within the range (0.85 – 1.2). The lift curve slope for transonic flow may be estimated by the conventional method, (fig. (1)) namely, by matching the slopes for subsonic and supersonic flows and after that down to reduced the distance between these slopes [9]. In recent years finite difference methods have been quite widely used for the calculation of transonic flow. Andreas sommerer, [1], showed transonic flow over airfoil , E .Krause,W.Jager(eds.), [2], calculated transonic flow past unswept and swept wings P.M.Congedo,C.Corre,P.Cinnella.,[3] , comprised shock wave over transonic airfoil. And Jameson. ,[4] studied efficient aerodynamic shape optimization . In the present work the, aerodynamic parameters of swept and unswept wings in the transonic flow regime are investigated.

2- Method of Analysis

2-1 Transonic flow past a NACA0012 airfoil

The transonic potential flow equation, which may be derived from the Euler equations for the inviscid compressible flow introducing the assumption that the flow is irrotational, so that a velocity potential φ can be defined. Shock waves can be expected to appear the profile is specially designed to prevent their formation. Since an irrotational flow is isentropic, the introduction of a potential implies that shock waves are to be replaced by discontinuities across which the entropy is conserved.

The Euler equations are [10]:

$$\frac{\partial \omega}{\partial t}+\frac{\partial f}{\partial x}+\frac{\partial g}{\partial y}=0 \qquad \ldots. (1)$$

Consider a two dimensional flow past an airfoil, Let u, v and q be the velocity components and speed

$$\mathcal{U} = \phi_z,\ \mathcal{V} = \phi_y \text{and}$$
$$q = \sqrt{\mathcal{U}^2 + \mathcal{V}^2} \quad \ldots.(2)$$

The Euler equations now reduce to the potential flow equation

$$\frac{\partial}{\partial x}(\rho\phi_x) + \frac{\partial}{\partial y}(\rho\phi_x) = 0 \quad \ldots. (3)$$

and let a be the local speed of sound. Then φ is to be determined from the quasilinear equation

$$(a^2 - \mathcal{U}^2)\,\phi_{xx} - 2\mathcal{U}\mathcal{V}\phi_{xy} + (a^2 - \mathcal{U}^2)\phi_{yy} = 0 \quad \ldots\ldots (4)$$

Which is hyperbolic if the local Mach number M = q/a > 1, and elliptic if M < 1. At the profile

the solution should satisfy the Neumann boundary condition

$$\frac{\partial \phi}{\partial n} = 0 \quad \ldots\ldots. (5)$$

Where n denotes the normal direction. At infinity the solution should approach a uniform free stream with a speed q_∞ and Mach number M_∞ . The local speed of sound can be determined from the energy equation

$$a^2 + \frac{\gamma-1}{2}q^2 = \left(\frac{1}{M_\infty^2} + \frac{\gamma-1}{2}\right) q_\infty^2 \quad \ldots\ldots..(6)$$

Here γ is the ratio of specific heats. The density ρ and pressure p follow from the relations

$$\rho^{\gamma-1} = M_\infty^2\, a^2 \quad \ldots.. (7)$$

$$p = \frac{\rho^2}{\gamma\, M_\infty^2} \quad \ldots\ldots (8)$$

Because shock waves generate entropy, they cannot be exactly modeled by the potential flow equation. Weak solutions admitting isentropic jumps which conserve mass but not momentum are a good approximation to shock waves, however, as long as the shock waves are quite weak (with a Mach number < 1.3 for the normal velocity component upstream of the shockwave). Stronger shock waves tend to separate the flow, with the result that the inviscid approximation is no longer adequate. Thus this model is well balanced, and it has proved extremely useful for estimating the cruising performance of transport aircraft. If one assumes small disturbances and a Mach number close to unity, the potential equation can be reduced to the transonic small disturbance equation. A typical form is

$$(1 - \mathrm{M}_\infty^2 - (\gamma+1)\mathrm{M}_\infty^2\,\phi_X)\phi_{XX} + \phi_{YY} = 0 \quad \ldots.. (9)$$

Finally, if the free stream Mach number is not close to unity, the potential flow equation can be linear zed as

$$(1 - \mathrm{M}_\infty^2)\phi_{XX} + \phi_{YY} = 0 \quad \ldots.. (10)$$

By using Visual Foil Plus the pressure distribution and lift coefficient and Mach contours for flow Past a NACA 0012 airfoil can be predicted.

2-2 Critical Mach number: -

As subsonic air flow over an airfoil (or wing), it accelerates, reaches a maximum speed and then decelerates toward the trailing edge

Since T_o= constant,

$$T = T_0 - \frac{u^2}{2C_P} = T_0 - \frac{u^2 r-1}{2R\gamma} \ldots(11)$$

Thus, the Mach number of the flow increases and then decreases. The magnitude of this Change depends on the airfoil shape and the angle of attack. Thus, it is evident that, as you. Increase M∞, the highest local M on the surface may exceed 1 long before reaches M∞. The value of M∞ at which the highest M on the airfoil first reaches 1 is called the critical Mach number M_{Cr} . [11]

Knowing that

$$\frac{P}{P_0} = (1 + \frac{\gamma-1}{2} M^2)^{\frac{\gamma}{1-\gamma}} \quad \ldots\ldots (12)$$

For Isentropic flows relation

$$\frac{P_\infty}{P_0} = (1 + \frac{\gamma-1}{2} M_\infty^2)^{\frac{\gamma}{1-\gamma}} \quad \ldots.. (13)$$

Or

$$\frac{P-P_\infty}{\frac{\gamma}{2}M_\infty^2 P_\infty} \equiv C_P = \frac{2}{\gamma M_\infty^2}(\frac{P}{P_\infty} - 1) \quad \ldots\ldots.(14)$$

Therefore

$$C_P = \frac{2}{\frac{\gamma}{2}M_\infty^2}[(\frac{1+\frac{\gamma-1}{2}M^2}{1+\frac{\gamma-1}{2}M_\infty^2})^{\frac{\gamma}{1-\gamma}} -] \quad \ldots\ldots.(15)$$

At$M_\infty = M_{Cr}$, M reaches 1 somewhere. The value of C_P at this point can be

Found by setting M=1

$$C_P = \frac{2}{\gamma M_\infty^2}[(\frac{\frac{\gamma+1}{2}}{1+\frac{\gamma-1}{2}M_{\infty cr}^2})^{\frac{\gamma}{1-\gamma}} - 1] \quad \ldots\ldots(16)$$

2-3 Supercritical Airfoils

The preceding discussion shows that if $M_\infty > M_{Cr}$ drag is greatly raised, how matter Mcr can be increased, very thin airfoil with a sharp leading edge may be used, this is impractical for airliners. By reducing the curvature on the upper surface, therefore this reduction can lead to decelerate the flow over airfoil, so that any shock formed will be relatively weak. Figure 16. Shows the differential C_P and shock wave location over airfoil and supercritical airfoil. [12]

2-4 Swept wing

The effect of swept wing angle (Λ) on C_L slope and induced drag. C_L of awing is given by [9]

$$C_L = \frac{2\pi A}{2+\sqrt{4+\frac{A^2\beta^2}{\eta^2}\left[1+\frac{tan^2 \Lambda_{maxt}}{\beta^2}\right]}} \quad \ldots\ldots. (17)$$

Where

$\beta^2 = -M^2$, η = C_L / (2π / β) and Λ : sweep back wing angle $(\Lambda)_{maxt}$= sweep of the line of maximum thickness C_L is the slope of lift curve of the airfoil used on wing at chosen flight Mach number. In the absence of this information, η can be taken as 1. From Eq. (17) it is seen that C_L decreases as sweep increases.

Based on experimental data on swept wing, [5] [6] the induced drag of a swept wing is inversely proportional to cosine of (Λ-5^o) i.e.

$$C_{Di} \propto \frac{1}{\cos(\Lambda - 5^{o})} \quad \text{..... (18)}$$

$$C_{d} = \frac{1}{\sqrt{M_{\infty}^{2} - 1}} \quad \text{.....(19)}$$

However when the critical Mach number is exceeded unity, the drag coefficient starts to increase. Making use of this behavior we define the term 'Drag divergence Mach number (M_{DD})' as the Mach number at which the slope of the C_D vs. M curve has a value of 0.1 i.e. (d C_D/ dM) = 0.1. [7] . For a swept wing the change in drag divergence Mach number due to sweep angle(Λ), is given by the following equation:-

$$\frac{1-(M_{DD})_{\Lambda}}{1-(M_{DD})_{\Lambda=0}} = 1 - \frac{\Lambda}{90} \quad \text{.....(20)}$$

Where $(M_{DD})_{\Lambda=0}$ and$(M_{DD})_{\Lambda}$ are the drag divergence Mach numbers of the unswept and the swept wings respectively, (Λ) is quarter-chord sweep in degrees.

3- Results and Discussion

Figure (2) shows the calculated Mach number contours around NACA0012 airfoil at free stream Mach number (0.5). The flow around the airfoil is subsonic. The slope of the lift curve as indicated in fig. (1) Is approximately (9/rad). The flow field measurements about supercritical airfoil section given by Hurley, etal. [12] is shown in fig. (3). Good qualitative agreement between the present results (fig.2) and measurement (fig.3) is obtained. The calculated Euler and potential flow pressure distributions on NACA0012 airfoil at (*M∞=0.5)* are shown in fig. (4). The two solutions are identical over almost all the section surface.

Figure (5) shows the calculated Mach number contours around NACA0012 airfoil at (*M∞=0.8).*The flow is supersonic over nearly the entire upper surface and deceleration to subsonic speed occurs through a shock wave near the trailing edge. The lift is drastically reduced. Separation at the foot of the shockwave is more conspicuous and the turbulent wake is wide. Good qualitative agreement is obtained between the present results (fig.5) and measurements [12] (fig.6). Fig. (7) illustrates the pressure distribution over NACA0012 airfoil at (*M∞=0.8).*The compressible pressure coefficient (Euler results) is radically different than the potential theory results on both the upper and lower surface of the airfoil.

At free stream Mach number (*M∞=1.0),* the shock waves both for the upper and lower surface have reached the trailing edge, as shown in fig.(8). The local Mach number is supersonic for most of the airfoil surface. The lift curve slope wills increase as indicated in fig. (1).When the Mach number equal to (1.6) the free-stream flow is supersonic, a bow shock wave (i.e., the detached shock wave in front of the leading edge) is generated as shown in fig. (10).The flow around the airfoil is supersonic everywhere except very near the rounded nose. The shock waves at the trailing edge remain, but they have become weaker. The lift curve slope wills decrease as indicated in fig. (1). The Euler results for the pressure distribution are shown in figures (9) and (11).The subsonic potential theory can no longer predict the pressure coefficient

at Mach number equal to unity or higher. Figure (12) indicated the differential $C_p$and shock wave location over NACA0012 airfoil and supercritical airfoil [16]. Note, such airfoil were among the first to be designed using detailed mathematical computation comparison of transonic flow over usual NACA0012 and supercritical airfoils.

Figure(13) indicated the flow past unswept and swept wings, the difference between the critical Mach number for the unswept wing (=0.7) and the critical Mach number for the swept wing with sweep angle (35 deg.) (=0.85).That's mean the shock wave generated on the unswept wing at $M_{cr} = 0.7$ and it's generated on the swept wing at$M_{cr} = 0.85$. Finally, fig. (14) Shows the drag coefficient vs. Mach number [9]. Figure (15) shows the flow chart for Visual foil pulse software.

4-Conclusions

The transonic flow past unswept and swept wings has been studied. The velocity field and pressure coefficients are estimated as function of free stream Mach number. The results show the effect of free stream Mach number on shock waves location and the velocity field around the wing section. The Euler solution and potential flow solutions are identical at subsonic flow; however, at supersonic flow the potential theory can no longer predict the flow field correctly. The results show the important effect of sweep angle on the value of the critical Mach number for wings. By using Visual foil plus the pressure distribution and lift coefficient and Mach contours for flow Past a NACA 0012 airfoil can be predicted.

5-References

[1] Andreas Sommerer, Thorsten Lutz and Siegfried Wagner: Numerical optimization of Adaptive Transonic Airfoils with Variable Camber. In: Proceedings of the 22nd International Congress of the Aeronautical Sciences, 27 August – 1 September, 2000, Harrogate, UK, 2000.

[2] E. Krause, W. Jäager (eds.): High performance computing in science and engineering '02. Transaction of the high performance computing center Stuttgart (HLRS). Springer 2002.

[3] P.M. Congedo, C. Corre, P. Cinnella, 2005,"Airfoil shape optimization for transonic flows of Bethe-Zel'dovich-Thompson fluids". Accepted for publication in AIAA Journal.

[4] Jameson. Efficient aerodynamic shape optimization. AIAA Paper 2004-4369, 2004.

[5] Grasmeyer, J.M., "A Discrete Vortex Method for Calculating the Minimum Induced Drag
and Optimum Load Distribution for Aircraft Configurations with Noncoplanar Surfaces,"
VPI-AOE-242, Department of Aerospace and Ocean Engineering, Virginia Polytechnic
Institute and State University, Blacksburg, Virginia, 24061, January, 1997.

[6] Hoerner S.F. '' Fluid-dynamic drag '', published by Herner Fluid Dynamics, Brick Town ,NJ ,1965.

[7]Shevel , Richards , ; Bayan, Fawzi,P,; *Development of a method for predicting the drag divergence Mach number and the drag due to compressibility for conventional and supercritical wings* .Stanford, A, Stanford university , Department of Aeronautics and Astronautics,

Research Report SUDAAR 522,1980.-URL: http:// dlib.stanford .edu :6520/text 1/dd-ill/drag-divergence,PDF(2005-O2-25).

[8] Herner S.F.''Fluid –dynamic drag'',published by Hoerner fluid dynamic,Brick Town,NJ,1965.

[9]Daniel P Raymer. '' Aircraft Design: A Conceptual Approach '' Published by: American Institute of Aeronautics and Astronautics, Inc. 370 L'Enfant Promenade, S.W., Washington, D.C.20024.

[10]Antony Jameson. '' Transonic Flow Calculations'' Princeton University, MAE Report
=1651, December 7, 2003.

[11]James E.John., Theo G. Keith. '' Gas Dynamics'' Third Edition, Printed in the United States of America.2006.

[12]Hurley, F.X., F.W. Spaid.,F.W. Roos,L.S.Stivers, Jr., andA.Bandettini,''Detailed Transonic Flow Field Measurements about a Supercritical Airfoil Section,'' TMX-3244, NASA, July 1975.

[13] D.J.Kirshman.F.lio. ''Agridbless boundary condition method for the solution of the Euler regulations on embedded Cartesian meshes with multigrid.'' Page: 136,139. 2004.

[14] Simona Ciornei ''Mach number, relative thickness, sweep and lift coefficient of the wing ''page 34.2005

[15] Georg May., Balaji Srinivasan, Antony Jameson ''an improved gas-kinetic BGK finite-volume method for three-dimensional transonic flow'' page 872. 2006.

[16] Ayers,T.G.,''Supercritical Aerodynamics:Worth while over a Range of speeds''*Astronautics and Aeronautics* . Aug.1972.Vol,10,NO.8PP32-36.

[17] Anderson, J.D., S.Corda, and D.M.Van Wie, ''effect of swept wing on critical Mach number '' 1989. Page 226.

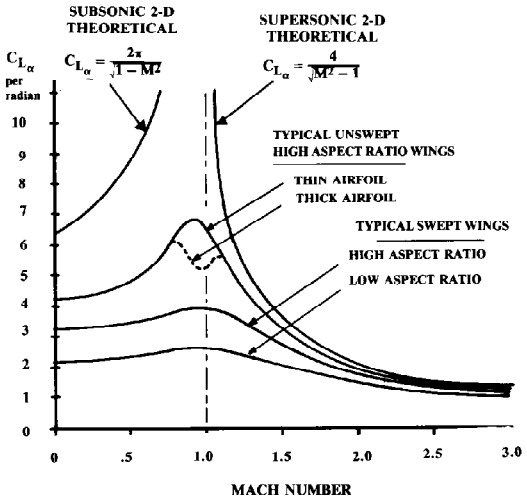


Figure (1) Lift curve slope as a function of Mach number [9]

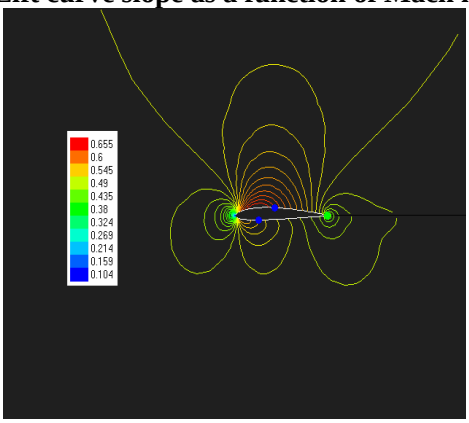


Figure (2) Calculated Mach number contours around NACA0012 Airfoil ($M\infty = 0.5$).

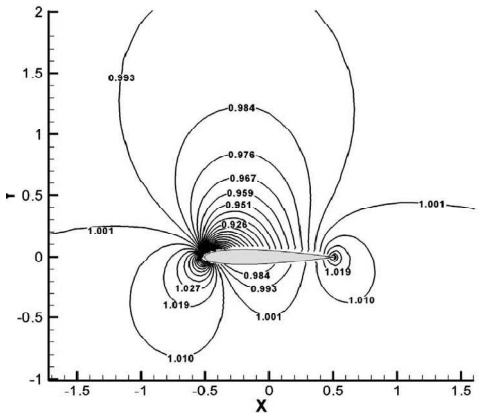


Figure (3) Measured Mach number contours around supercritical airfoil (M∞ = 0.5). [12]

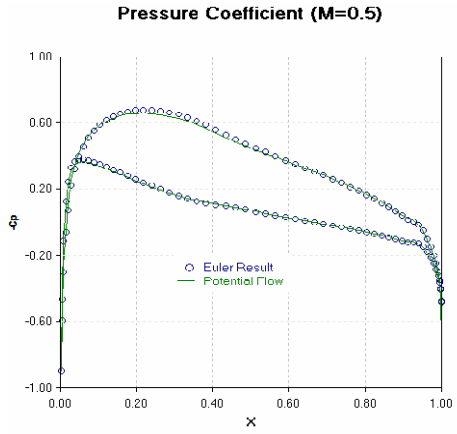


Figure (4) Pressure distribution on NACA0012 airfoil (M = 0.5).

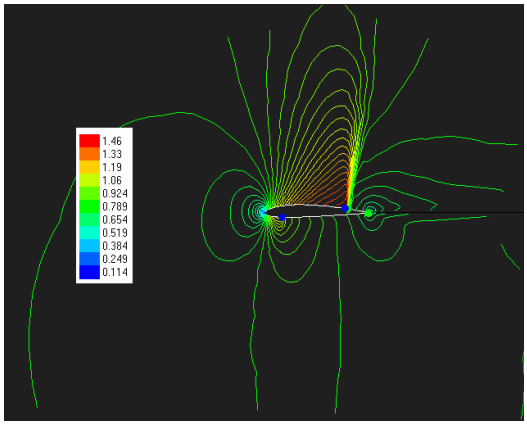


Figure (5) Calculated Mach number contours around NACA0012 airfoil (M∞ = 0.8).

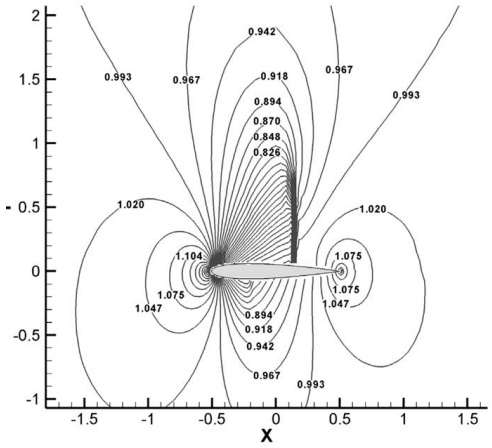


Figure (6) Measured Mach number contours around supercritical airfoil (M∞ = 0.8). [12]

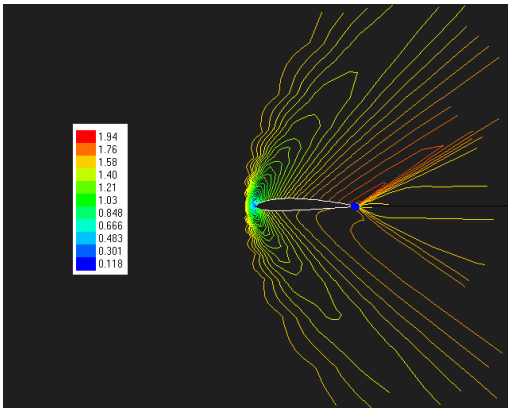


Figure (8) Calculated Mach number contours around NACA0012 airfoil (M∞ = 1.0).

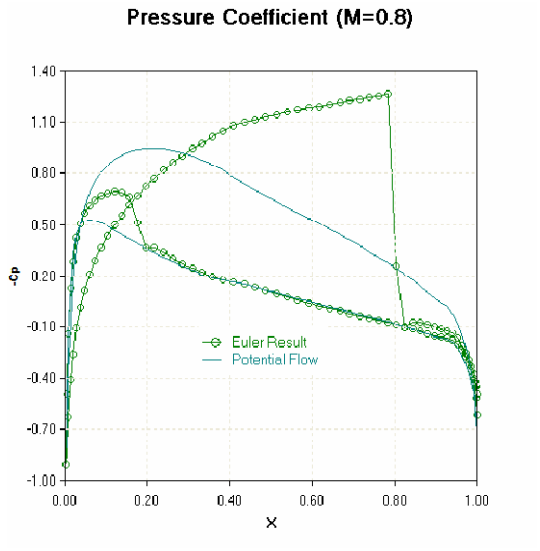


Figure (7) Pressure distribution on NACA0012 airfoil (M = 0.8).

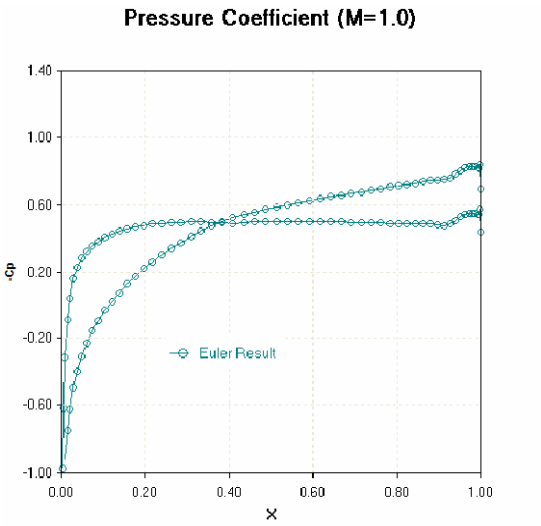


Figure (9) Pressure distribution on NACA0012 airfoil (M =1.0).

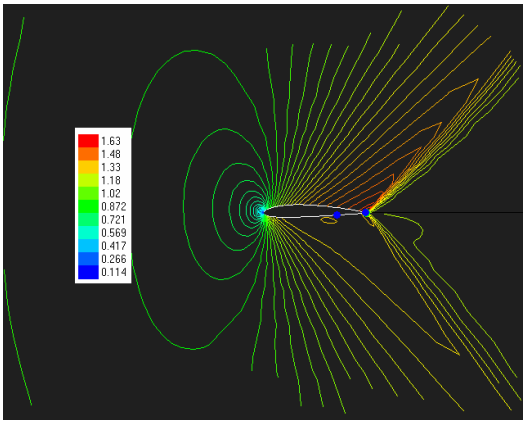


Figure (10) Calculated Mach number contours around NACA0012 airfoil (M∞ = 1.2)

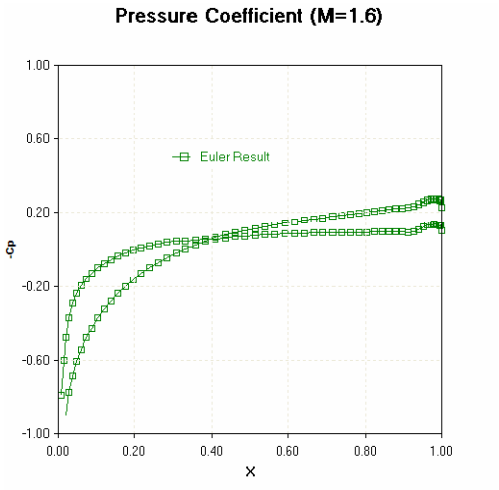
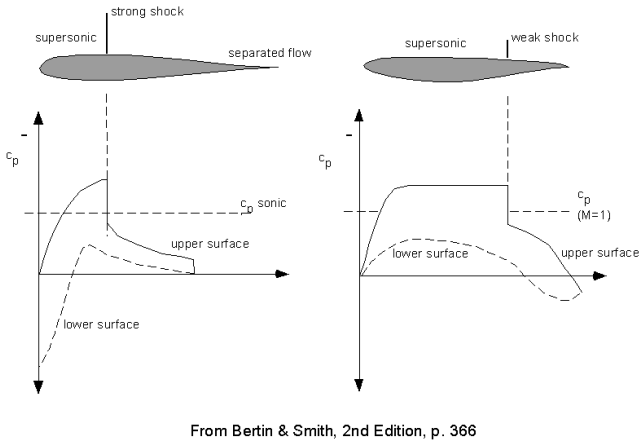


Figure (11) Pressure distribution on NACA0012 airfoil (M =1.2)



A.NACA0012 airfoil b. Supercritical airfoil SC (2)-0410

Figure (12) Differential C_P and shock wave location over a. NACA0012 airfoil and b. supercritical Airfoil SC (2)-0410 [16]

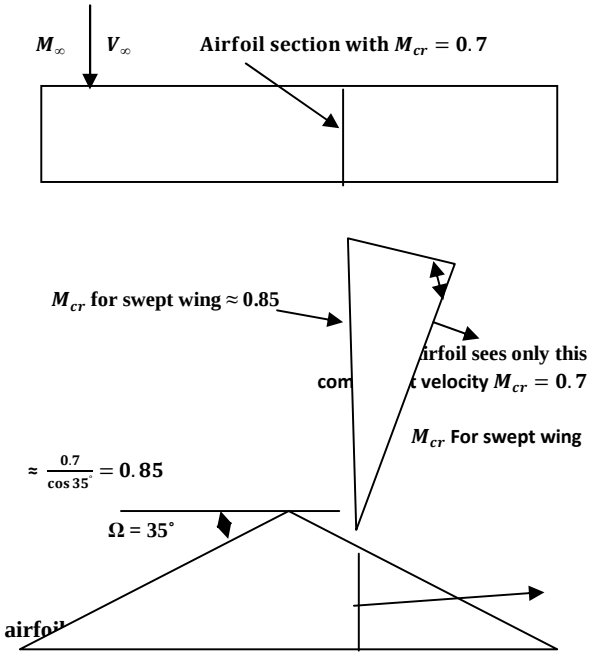


Figure (13) Flow past unsweep and a sweep wing [17]

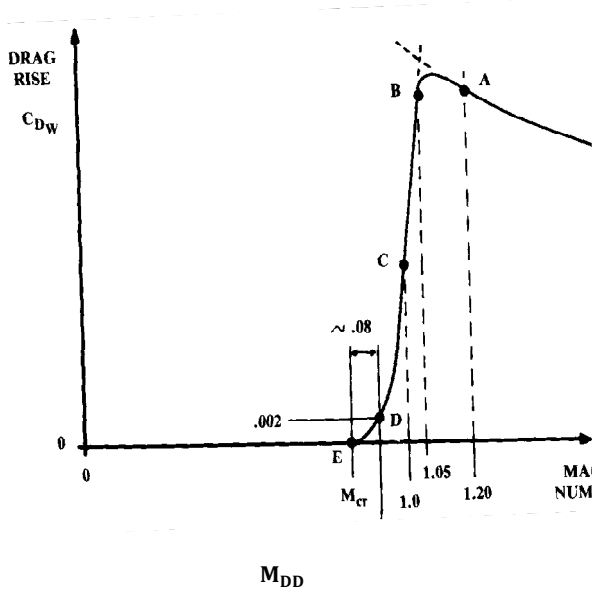


Figure (14) Drag coefficient vs. free-stream Mach number [9]

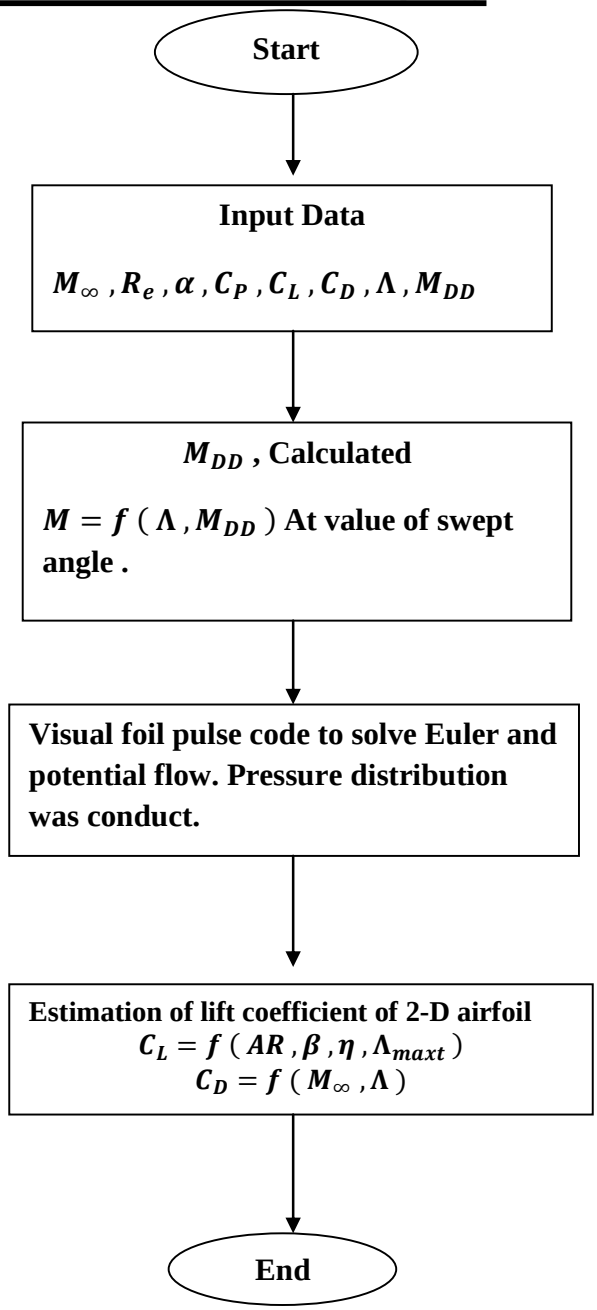


Figure (15) Flow chart for Visual foil pulse